Available online at www.sciencedirect.com
ScienceDirect
Biosensors and Bioelectronics 22 (2007) 2989–2993
BIOSENSORS & BIOELECTRONICS
www.elsevier.com/locate/bios

Glucose biosensor based on nano-SiO_2 and "unprotected" Pt nanoclusters

Haipeng Yang [a,b], Yongfa Zhu [a,*]

[a] *Department of Chemistry, Tsinghua University, Beijing 100084, PR China*
[b] *College of Materials Science and Engineering, Shenzhen University, Shenzhen Key Laboratory of Special Functional Materials, Shenzhen 518060, PR China*

Received 2 August 2006; received in revised form 10 December 2006; accepted 12 December 2006
Available online 27 December 2006

Abstract

The "unprotected" Pt nanoclusters (average size 2 nm) mixed with the nanoscale SiO_2 particles (average size 13 nm) were used as a glucose oxidase immobilization carrier to fabricate the amperometric glucose biosensor. The bioactivity of glucose oxidase (GOx) immobilized on the composite was maintained and the as-prepared biosensor demonstrated high sensitivity (3.85 $\mu A\,mM^{-1}$) and good stability in glucose solution. The Pt–SiO_2 biosensor showed a detection limit of 1.5 μM with a linear range from 0.27 to 4.08 mM. In addition, the biosensor can be operated under wide pH range (pH 4.9–7.5) without great changes in its sensitivity. Cyclic voltammetry measurements showed a mixed controlled electrode reaction.

Keywords: "Unprotected" Pt nanoclusters; Glucose oxidase; Glucose biosensor; Nanoscale SiO_2

1. Introduction

Glucose sensors have been developed greatly because of its high practical relevance of glucose determinations (Bakker, 2004). Among these sensors, considerable interests have been attracted by amperometric biosensors that based on immobilized glucose oxidase (GOx) (Prodromidis and Karayannis, 2002). Glucose biosensors utilizing immobilized oxidase for the conversion of the target analyte into electrochemically detectable products are one of the most widely used detection methods (Yang et al., 2004; Kros et al., 2001; Xian et al., 2006).

The methods of enzyme immobilization on electrodes include physical adsorption, cross-linked, covalent bonded, embed (enzyme into gels, cross-linked polymers), electrochemical deposition, electrostatic adsorption, etc. Recently nanoparticles enhancing enzyme immobilization technique has become widespread. Many kinds of nanoscale particles such as Au (Xian et al., 2006; Xiao et al., 2003), Pt and SiO_2 (Simonian et al., 2005; Selvaraju and Ramaraj, 2005; Luo et al., 2004; Yang et al., 2006), have been used to construct nano-biosensors. A variety of glucose biosensors with high sensitivity and excellent reproducibility based on nano technology have been reported (Yu and Ju, 2002; Wang and Musameh, 2003; Lin et al., 2004; Hrapovic et al., 2004; Liu and Lin, 2006; Liu et al., 2005; Zhang et al., 2004). However, the role of nanoparticles in the bio-system is not clear so far. In our previous work, it was reported that the nonmetallic nanoparticles increased the amperometric response by increasing the surface enzyme loading on the high surface area of nanosized particles (Yang and Zhu, 2005, 2006). In the present work, the role of metal nanoparticles in the biosensors was examined carefully.

The studies of Pt-based metal nanoparticles have been very active with the growing interest in building advanced materials such as fuel cells (Ding et al., 2005). Various methods are used for the preparation of nanosized Pt particles. In particular, Pt particle is prepared as colloidal solutions. To stabilize the colloids in solution, organic stabilizers such as polyvinyl pyrolidine that interact with Pt surface sites have been used widely (Dalmia et al., 1998; Bonet et al., 1999). However, the stabilizer molecules have to be removed as they hinder the active sites of Pt particles (Dubeau et al., 2003).

Wang and co-workers prepared "unprotected" nanoparticles of Pt with small particle size in organic media in the absence of any usual protective agent by heating corresponding metal hydroxide colloids in ethylene glycol containing NaOH for the

* Corresponding author. Tel.: +86 10 62783586; fax: +86 10 62787601.
E-mail address: zhuyf@mail.tsinghua.edu.cn (Y. Zhu).

0956-5663/$ – see front matter © 2007 Elsevier B.V. All rights reserved.
doi:10.1016/j.bios.2006.12.019

first time (Wang et al., 2000). This stable colloidal solution of Pt was obtained under basic conditions without adding PVP. The reaction mechanism was distinguished by Bock et al. (2004). In this way, a close contact of the metal nanoparticles with their supports could be achieved when these nanoscopic building blocks were used to assemble other functional materials. This advantage leads to the widespread applications of the "unprotected" nanoparticles (Wang et al., 2005). Here this kind of Pt nanoparticles mixed with nanosized silicon oxide was used as supporting materials of glucose oxidase to construct glucose biosensor. The relationship between Pt and immobilized enzyme, which is closely contact with each other without any organic stabilizers, was studied carefully by adjusting the ratio of Pt and SiO_2. High performance nanoparticle enhanced biosensors can be constructed by clarifying the role of nanoparticles in the biosensor.

2. Experimental

2.1. Chemicals and reagents

Glucose oxidase (GOx) was purchased from sigma company, the activity was 178.5 units mg^{-1}. β-D-Glucose and other chemicals used in this work were available with analytical reagent grade. Electrochemistry measurements were carried out in a 0.1 M phosphate buffer solution (pH 7.2), which was prepared by dissolving 0.061 mol di-sodium hydrogen phosphate and 0.039 mol sodium di-hydrogen phosphate in 1 L of double distilled water. Different stock concentrations of β-D-glucose were prepared in the buffer (0.1 M, pH 7.2) and stored at 4 °C when not in use (mutarotation was allowed for at least 12 h before using). All aqueous solutions were prepared using deionized water (18 MΩ cm). GOx was dissolved in phosphate buffer (0.1 M, pH 7.2) with a concentration of 4.0 mg mL^{-1} and stored at 4 °C. Nanoscale SiO_2 particles (99.9%) were purchased from Beijing Century Science & Technology Development Co. Ltd. The particle size was 13 nm nominally. Organic solvents and the other chemicals were of an AR grade and used as received.

2.2. Instrumentation

Transmission electron microscopy (TEM) photographs were measured on a Hitachi H-800 electron microscopy. The accelerating voltage of electron beam was 120 kV. Samples for TEM measurements were prepared by placing a drop of diluted nanocluster solution on a copper grid coated by a polymer or carbon film. The average diameter of the particles was determined from the diameters of 30 nanoparticles found in an arbitrarily chosen area.

Cyclic voltammetry (CV) and amperometric measurements were performed by using CHI 660B electrochemical workstation. A three electrode cell with platinum wire as a counter electrode and a saturated calomel electrode (SCE) as reference electrode served for electrochemical measurements. All experiments were conducted at 25 ± 0.5 °C without special announcement.

2.3. Preparation of "unprotected" platinum nanoclusters

The "unprotected" platinum nanoclusters were prepared in Wang's lab and the fabrication method has been described in previous reports (Wang et al., 2000). Briefly, a glycol solution of NaOH (50 mL, 0.5 M) was added into a glycol solution of $H_2PtCl_6{\cdot}6H_2O$ (1.0 g, 1.93 mmol in 50 mL) with stirring to obtain a transparent yellow platinum hydroxide or oxide colloidal solution which was then heated at 160 °C for 3 h, with an Ar flow passing through the reaction system to take away water and organic byproducts. A transparent dark-brown homogeneous colloidal solution of the Pt metal nanocluster (Pt: 3.76 g L^{-1} glycol, 19.3 mmol L^{-1}) was obtained without any precipitate. The "unprotected" platinum nanocluster in glycol was precipitated by adding HCl acid (1 M) to obtain a black precipitate. A transparent, dark-brown colloidal solution were obtained by "dissolving" the precipitate in ethanol by ultrasonic.

2.4. Sensor fabrication

Platinum wire with a diameter of 0.7 mm was polished and cleaned as base electrode. The clean Pt electrode was then dipped into a Pt–SiO_2 composite, which was made by dropping platinum nanocluster solution into a mixture of SiO_2 nanoparticles and 1 mL 2% polyvinyl butyral (PVB) solution of ethanol with ultrasonic. The electrode was prepared by adding 0.5 mL of Pt_{nano} solution (3.76 mg mL^{-1}) and 20 mg of SiO_2 into 1 mL 2% PVB solution. Moreover, the amount of the SiO_2 nanoparticles was adjusted to optimize the Pt–Si ratio (e.g., 0, 5, 10 and 30 mg of SiO_2 particles have been added). About 15 min of sonication was required to get uniformly dispersed Pt–SiO_2 suspension. The bare Pt electrode was lifted up at a rate of 3 cm min^{-1} after 1 min of dipping and then dried in air for about 1 h. A 3 μL drop of glucose oxidase solution (4.0 mg mL^{-1}) was dried on the SiO_2–Pt modified electrode in 1 h. Then 3.5 μL of glutaraldehyde (2.5%) was dropped on the resulting electrode to cross-link the enzyme in 1–2 h. Lastly, the enzyme-modified electrode was coated with PVB by dipping into 2% PVB solution for about 1 min and lifting up at a rate of 3 cm min^{-1}. The resulted Pt_{nano}–SiO_2/GOx sensors were washed with phosphate buffer (0.1 M, pH 7.2) and stored at 4 °C. Cyclic voltammetry and amperometry were carried out in 0.1 M phosphate buffer (pH 7.2).

The active surface area of the electrodes prior to enzyme immobilization was determined by steady-state voltammetry in a solution of 20 mM $K_4Fe(CN)_6$ with 0.2 M potassium chloride as the supporting electrolyte.

3. Results and discussion

3.1. Electrochemical characterization of the modified electrode

The size of the nano-SiO_2 particles was confirmed to be 13 ± 4 nm (80%) by TEM micrographs. The distributed Pt nanoclusters own an average diameter of 1–2 nm (Wang et al., 2000).

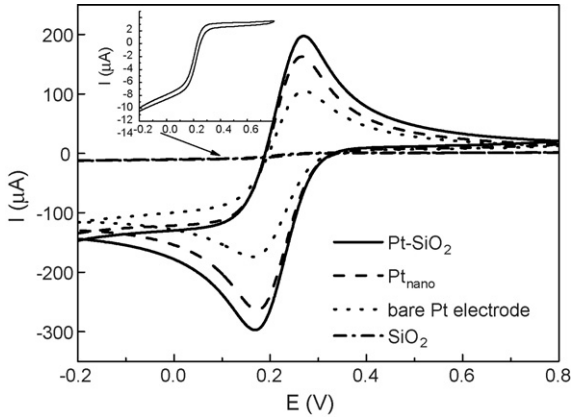

Fig. 1. The cyclic voltammetry curves of four different types of electrodes: Pt_{nano}–SiO_2, Pt_{nano}, SiO_2 modified electrode and the bare Pt electrode (20 mM $Fe(CN)_6^{4-}$ and 0.2 M KCl at 20 mV s^{-1}). The inset shows the enlarged curve of SiO_2 modified electrode.

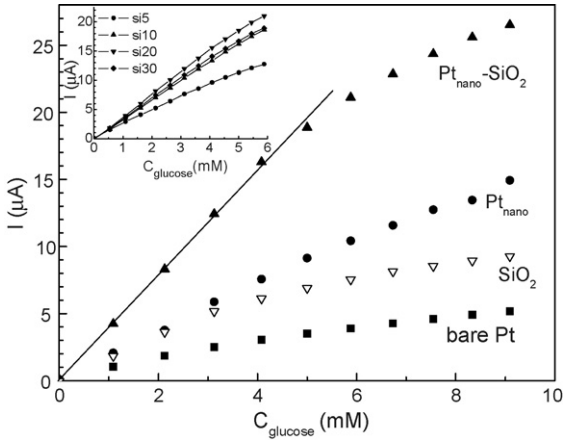

Fig. 2. Amperometric responses for Pt_{nano}–SiO_2/GOx, Pt_{nano}/GOx, SiO_2/GOx and bare Pt/GOx electrodes at different glucose concentrations in 0.1 M phosphate buffer (pH 7.2) at 0.6 V vs. SCE. The upper inset shows the influence of Pt–Si ratio on the response current of the biosensors (5, 10, 20 and 30 mg of SiO_2 with 1.88 mg Pt_{nano}, respectively).

The surface area of the bare Pt substrate electrode was 7 mm^2. The Pt electrode was calcined with alcohol burner before using. Calcining was an efficacious way to clean the surface of noble metal electrode. After calcining, it was found that the carbon atoms in the electrode surface reduced and the surface platinum atoms increased, which leads to high activity of the base Pt electrode (Yang and Zhu, 2005).

Cyclic voltammetry of ferrocyanide system is a valuable and convenient tool to monitor the characteristic of the surface of modified electrode (Walcarius, 2001). Cyclic voltammetry was conducted in 20 mM $Fe(CN)_6^{4-}$ and 0.2 M KCl at 20 mV s^{-1} for four different types of electrodes: Pt_{nano}–SiO_2, Pt_{nano}, SiO_2 modified electrode and the bare Pt electrode. Fig. 1 shows the steady-state CVs for the bare and the three modified Pt electrodes. For the bare Pt electrodes, the well-defined oxidation and reduction peaks caused by the Fe^{3+}/Fe^{2+} redox couples were noticed at +0.27 and +0.17 V versus SCE in forward and reverse scans, respectively. The peak current of Pt_{nano} and Pt_{nano}–SiO_2 modified electrode was increased because of the large surface area of nanoscale Pt dispersed in the modifying layer. According to Randles–Sevcik equation (Hrapovic et al., 2004):

$$I_p = 2.69 \times 10^5 A D^{1/2} n^{3/2} \gamma^{1/2} C$$

where A represents the area of the electrode (cm^2), n the number of electrons participating in the reaction, is equal to 1, D the diffusion coefficient of the molecule in solution, is $(6.70 \pm 0.02) \times 10^{-6}$ cm^2 s^{-1}, C the concentration of the probe molecule in the solution, is 20 mM, and γ is the scan rate (V s^{-1}). The Pt–SiO_2 electrodes exhibit the highest electroactive surface area, the average value of the electro active surface area for the optimized Pt_{nano}–SiO_2 electrode (1.88 mg Pt added into 20 mg of silicon dioxide) was 10.2 mm^2 compared with 5.3 mm^2 for the bare Pt electrode. The small peak current of SiO_2 modified electrode may be due to the insulation properties of the mixed film of nano-SiO_2 and PVB, which blocked the transfer of electrons between the solution and the base Pt electrode. The S shape's CV curve of SiO_2 modified electrode was shown in the inset of Fig. 1, indicating the bare Pt electrode becomes a microelectrode array by modifying films of nanoscale SiO_2 particles (Lin et al., 2004).

3.2. Effects of Pt and SiO_2 nanoparticles

GOx cross-linked with glutaraldehyde was immobilized on the modified electrode. The Pt–SiO_2/GOx electrode was tested by using a CHI660B electrochemical workstation. During chronoamperometric measurements, the working electrode was poised at +0.60 V versus SCE (Hrapovic et al., 2004). At each amperometric measurement, a certain amount of glucose was added into the system with stirring when the background current was stable (stirring rate: ~1000 rpm).

The I–C curves of Pt_{nano}–SiO_2/GOx, Pt_{nano}/Gox, SiO_2/Gox and bare Pt/GOx biosensors were shown in Fig. 2. The volume of enzyme on each biosensor was 3 μL (about 2.5 units). When the bare electrode was modified with Pt_{nano} or SiO_2, the response current increased. When the bare electrode was modified with mixed particles of Pt_{nano} and SiO_2, the response current increased greatly compared with simplex particles. The Pt_{nano}–SiO_2/GOx sensor could work linearly in glucose solution with a concentration range between 0.27 and 4.08 mM. The corresponding regression equation of the linear plot was: I (μA) = 0.026 + 3.98C, N = 5, S.D. = 1.13×10^{-7}, R = 0.9999, where C is the glucose concentration in mM. The sensitivity was thus estimated as 56.8 μA mM^{-1} cm^{-2} (3.98 μA mM^{-1}). While for the Pt_{nano}/Gox and SiO_2/Gox sensor, the corresponding regression equations in the same glucose concentration range were: I (μA) = 0.043 + 1.84C, N = 5, S.D. = 1.25×10^{-7}, R = 0.9993 and I (μA) = 0.151 + 1.54C, N = 5, S.D. = 3.07×10^{-7}, R = 0.995, respectively. The sensitivities were 26.3 μA mM^{-1} cm^{-2} (1.84 μA mM^{-1}) and 22.0 μA mM^{-1} cm^{-2} (1.54 μA mM^{-1}). For the bare Pt/GOx biosensor, the regression equation between 0.27 mM and 4.08 mM was: I (μA) = 0.182 + 0.73C, N = 5, S.D. = 1.26×10^{-7}, R = 0.995. The sensitivity was only 10.4 μA mM^{-1} cm^{-2} (0.73 μA mM^{-1}). For the optimization of

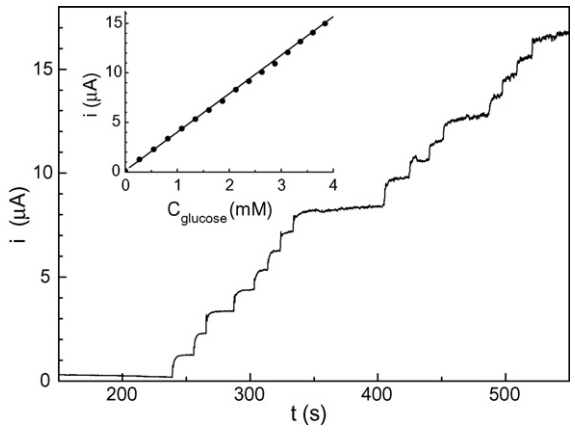

Fig. 3. Amperometric responses for Pt_{nano}–SiO_2/GOx electrode upon subsequent additions of 50 μL glucose solution (50 mM) in 0.1 M phosphate buffer (pH 7.2) at 0.6 V vs. SCE. Inset shows the calibration curve for glucose concentrations between 0.27 and 4.08 mM.

the Pt–Si ratio, the amount of SiO_2 nanoparticles was varied with constant platinum nanocluster solution. That is, experiments were carried out with 5, 10, 20 and 30 mg of SiO_2 with the constant amount of Pt_{nano} (1.88 mg). With the increase of SiO_2, the response current was increased firstly and then decreased. When 20 mg of SiO_2 was used, the highest response current was observed (see the inset in Fig. 2).

Under the optimal condition, well-defined amperometric responses for glucose were obtained at the Pt_{nano}–SiO_2/GOx biosensor. Fig. 3 displayed a typical amperometric response curve of the optimal Pt–SiO_2/GOx electrode (Pt 1.88 mg, SiO_2 20.0 mg). A stable and fast amperometric response could be observed with the successive injections of 50 μL glucose solution (50 mM) into phosphate buffer (0.1 M, pH 7.2). The time required to reach stable response was less than 3 s. The resulting calibration plot for glucose over the concentration range of 0.27–4.08 mM (considering the change of solution volume) was presented in upper inset. It indicated that such an electrode could work well in concentration range between 0.27 mM and 4.08 mM. The corresponding regression equation of the linear plot was: I (μA) = 0.09 + 3.85C, N = 17, S.D. = 1.21×10^{-7}, R = 0.9997. The sensitivity was thus estimated as 55.0 μA mM^{-1} cm^{-2} (3.85 μA mM^{-1}). The deviation of the response currents obtained here and previously (Fig. 2) is less than 4%, showing high reproducibility of the Pt_{nano}–SiO_2/GOx biosensor. Thus the error bars is less than 4% for each data. The detection limit (S/N = 3) were determined to be 1.5 μM.

3.3. Effect of pH

The investigation of the effect of pH value on the performance of biosensor is of great importance. The pH dependence of the sensor was evaluated at 2.5 mM glucose solution over the pH range from 4.1 to 8.3 (the response currents at different pH value were 6.28 μA with pH 4.1, 9.40 μA with pH 4.9, 9.28 μA with pH 5.3, 9.52 μA with pH 5.8, 9.79 μA with pH 6.4, 9.70 μA with pH 6.7, 9.76 μA with pH 7.2, 9.63 μA with pH 7.5 and 8.15 μA with pH 8.3, respectively). When pH of the buffer was very low or very high, GOx electrode exhibited low response current to glucose. However, the biosensor displayed pH independent in the pH range 4.9–7.5. In this pH range, the maximal responses current were almost the same, which is not in agreement with the relevant pH behavior reported elsewhere (Chen and Dong, 2003; Couto et al., 2002). Usually, the activity of native enzyme depends on pH strongly. In case of immobilization enzyme, though the pH shifting of maximal enzyme activity is often observed, its activity is still pH dependent (Li et al., 2001).

3.4. Electrochemical behaviors of the biosensor

Fig. 4A shows the cyclic voltammograms of Pt_{nano}–SiO_2/GOx sensor in 2.5 mM glucose solution with the sweep rate from 10 to 500 mV s^{-1}. Fig. 4B shows the corresponding fitting curves of peak current versus sweep rate (ν), the square root of sweep rate ($\nu^{1/2}$) and the three fourth power of sweep rate ($\nu^{3/4}$). In case that the peak current versus the square root of sweep rate plot was linear, it means a surface diffusion controlled process. In case that the peak current versus the sweep rate plot was linear, it means a surface-confined electrode reaction (Liu et al., 2005). As seen from Fig. 4B, neither the peak current versus the square root of sweep rate nor the peak current versus the sweep rate plot was linear, which indicates that the kinetic behavior of the biosensor is of mixed controlling.

The redox center ($FAD/FADH_2$) of GOx is deeply entrapped in the long chains of enzyme, which makes the distance from

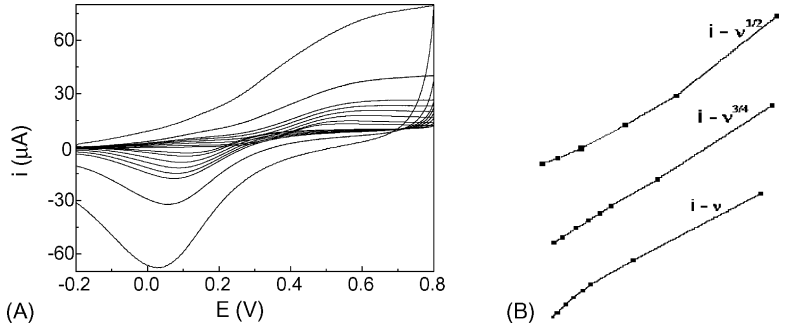

Fig. 4. (A) Cyclic voltammograms of Pt_{nano}–SiO_2/GOx sensor in 2.5 mM glucose at scan rates of: 10, 20, 40, 60, 80, 100, 200 and 500 mV s^{-1}. (B) Fitting curves of peak current vs. (i) sweep rate (ν), (ii) the square root of sweep rate ($\nu^{1/2}$) and (iii) the three-fourth power of sweep rate ($\nu^{3/4}$).

the electrode surface to the redox center farther than the distance that electrons can transfer at quick enough rates, and lead to a diffusion controlled process. In Pt_{nano}–SiO_2/GOx complex, the Pt nanoparticles (about 2 nm) are much smaller than the enzyme molecule (about 7 nm), and can act as good electrical conductors between the electrode and GOx. The electron transfer rate between GOx and the electrode is calculated as $1.70\,s^{-1}$ by method of Laviron (1979), it is higher than that of bare Pt/GOx biosensor ($0.87\,s^{-1}$) and SiO_2/GOx biosensor ($1.25\,s^{-1}$). Thus, the Pt nanoparticles mediate the electron transfer between the FAD sites and the base Pt electrode, which leads to fast electrochemical kinetics between the immobilized enzyme and the electrode, and make the system remarkable in its transduced current densities (Willner et al., 1996). The kinetic behavior of the biosensor changed from diffusion controlled process into the mixed process of diffusion controlled process and surface-confined electrode reaction. This may be related to the pH independence of the sensor. Since the Pt nanoparticles mediate electron transfer from the electrode to FAD sites, the changes of the conformation of the enzyme does not alter the distance from the electrode surface to FAD sites so drastically.

4. Conclusion

The present work demonstrates that it is possible to obtain glucose biosensors by entrapping GOx into the Pt_{nano}/SiO_2 composite matrix. The electron transfer rate of Pt_{nano}–SiO_2/GOx ($1.70\,s^{-1}$) is much higher than Pt/GOx biosensor ($0.87\,s^{-1}$) and SiO_2/GOx biosensor ($1.21\,s^{-1}$). This may be caused by the small Pt nanoclusters which mediating the electron transfer between the electrode and the GOx. The optimized Pt_{nano}–SiO_2/GOx biosensor displays high sensitivity ($3.85\,\mu A\,mM^{-1}$) with a linear range from 0.27 to 4.08 mM in glucose solution, and is pH independent from pH 4.9 to 7.5. This composite structure provides promising electrode materials for the development of biosensors, biofuel cells and other bioelectrochemical devices.

Acknowledgement

This work was partly supported by Chinese National Science Foundation (20433010, 20571047).

References

Bakker, E., 2004. Anal. Chem. 76, 3285–3298.
Bock, C., Paquet, C., Couillard, M., Botton, G.A., MacDougall, B.R., 2004. J. Am. Chem. Soc. 126, 8028–8037.
Bonet, F., Delmas, V., Grugeon, S., Urbina, R.H., Silvert, P.Y., Tekaia-Elhsissen, K., 1999. Nanostruct. Mater. 11, 1277–1284.
Chen, X., Dong, S., 2003. Biosens. Bioelectron. 18, 999–1004.
Couto, C., Araújo, A., Montenegro, M., Rohwedder, J., Raimundo, I., Pasquini, C., 2002. Talanta 56, 997–1003.
Dalmia, A., Lineken, C.L., Savinell, R.F., 1998. Colloid Interf. Sci. 205, 535–537.
Ding, J., Chan, K., Ren, J., Xiao, F., 2005. Electrochim. Acta 50, 3131–3141.
Dubeau, L., Coutanceau, C., Garnier, E., Leger, J.M., Lamy, C., 2003. J. Appl. Electrochem. 33, 419–429.
Hrapovic, S., Liu, Y., Male, K.B., Luong, J.H.T., 2004. Anal. Chem. 76, 1083–1088.
Kros, A., Gerritsen, M., Sprakel, V., Sommerdijk, N., Jansen, J., Nolte, R., 2001. Sensor Actuat. B 81, 68–75.
Laviron, E., 1979. J. Electroanal. Chem. 101, 19–28.
Li, Q., Luo, G., Feng, J., Zhou, Q., Zhang, L., Zhu, Y., 2001. Electroanalysis 13, 413–416.
Lin, Y., Lu, F., Tu, Y., Ren, Z., 2004. Nano Lett. 4, 191–195.
Liu, G., Lin, Y., 2006. Electrochem. Commun. 8, 251–256.
Liu, Y., Wang, M., Zhao, F., Xu, Z., Dong, S., 2005. Biosens. Bioelectron. 21, 984–988.
Luo, X., Xu, J., Zhao, W., Chen, H., 2004. Sensor Actuat. B 97, 249–255.
Prodromidis, M.I., Karayannis, M.I., 2002. Electroanalysis 14, 241–261.
Simonian, A.L., Good, T.A., Wang, S.S., Wild, J.R., 2005. Anal. Chim. Acta 534, 69–77.
Selvaraju, T., Ramaraj, R., 2005. J. Electroanal. Chem. 585, 290–300.
Walcarius, A., 2001. Electroanalysis 13, 701–718.
Wang, J., Musameh, M., 2003. Anal. Chem. 75, 2075–2079.
Wang, Y., Ren, J., Deng, K., Gui, L., Tang, Y., 2000. Chem. Mater. 12, 1622–1627.
Wang, Y., Zhang, J., Wang, X., Ren, J., Zuo, B., Tang, Y., 2005. Top. Catal. 35, 35–41.
Willner, I., Heleg-Shabtai, V., Blonder, R., Katz, E., Tao, G., Bückmann, A., Heller, A., 1996. J. Am. Chem. Soc. 118, 10321–10322.
Xian, Y., Hu, Y., Liu, F., Xian, Y., Wang, H., Jin, L., 2006. Biosens. Bioelectron. 21, 1996–2000.
Xiao, Y., Patolsky, F., Katz, E., Hainfeld, J., Willner, I., 2003. Science 299, 1877–1881.
Yang, Y.H., Yang, H.F., Yang, M.H., Liu, Y.L., Shen, G.L., Yu, R.Q., 2004. Anal. Chim. Acta 525, 213–220.
Yang, H., Zhu, Y., 2006. Talanta 68, 569–574.
Yang, H., Zhu, Y., 2005. Anal. Chim. Acta 554, 92–97.
Yang, M., Yang, Y., Liu, Y., Shen, G., Yu, R., 2006. Biosens. Bioelectron. 21, 1125–1131.
Yu, J., Ju, H., 2002. Anal. Chem. 74, 3579–3583.
Zhang, M., Smith, A., Gorski, W., 2004. Anal. Chem. 76, 5045–5050.